



## Characterization of PVVH/PEMA blend polymer with gold nanoparticles as corrosion inhibitors for N80 carbon steel in a 5% sulfamic acid solutions

A.Y. Yassin <sup>1</sup>, Y.M. Abdallah <sup>1</sup>

<sup>1</sup> Department of Basic Sciences, Delta University for Science and Technology, Gamasa, Mansoura, Egypt, 11152.

\* **Correspondence:** Department of Basic Sciences, Delta University for Science and Technology, Gamasa, Mansoura, Egypt, E-mail address: [dr.ymostafa8@gmail.com](mailto:dr.ymostafa8@gmail.com), [Yasser\\_mostafa@deltauniv.edu.eg](mailto:Yasser_mostafa@deltauniv.edu.eg) (Y.M. Abdallah).

### ABSTRACT

In this study, we used the solution casting approach to create a polymer mix of Poly (vinyl chloride-co-vinyl acetate-co-2-hydroxypropyl acrylate) and Poly (ethyl methacrylate) (PEMA), which we subsequently filled with 3 wt % of gold nanoparticles (Au-NPs). By electrochemical procedures such electrochemical impedance spectroscopy (EIS), the present composite was used as corrosion inhibitors for N80 carbon steel in 5 % sulfamic acid solutions. The DFT technique used quantum chemical computations to establish an acceptable theoretical interpretation for the composite's adsorption and inhibition performance on the carbon steel surface. In the case of blend 3% Au-NPs, the inhibition productivity climbs to 89 % when the concentrations are increased to  $5 \times 10^{-4}$  M. It was discussed as it relates to the nanocomposite's adsorption on the steel metal surface, which was confirmed using SEM. The total impedance increased as the studied polymer concentration increased, and the continual addition to the phase angle move was clearly connected with the growing of the investigated polymer concentration adsorbed on carbon steel species, according to Bode plots. The quantum chemical variables (DFT and Mulliken atomic charges) and experimental computations had a significant agreement, confirming the nanocomposite's efficacy as corrosion inhibitors.

**Keywords:** PVVH/PEMA blend; gold nanoparticles; corrosion; XRD; EIS; DFT.

### 1. Introduction

Nanoparticles' significance stems from their prospective applications in a variety of sectors, including medicine, biology, physics, and chemistry. Due to its exceptional features, such as high surface area, optical, surface plasmon resonance (SPR), electrical, and biological properties, gold nanoparticles are one of the most important metallic nanoparticles (Mubarak Ali et al. 2011). The laser ablation technique has recently been utilised to synthesise Au-NPs in liquids, allowing them to be uniformly dispersed and characterised by a variety of morphologies, such as nanospheres, nanowires, and irregular shapes (Farea et al., 2020).

Corrosion, a naturally occurring process in metals, poses a severe threat to corporate and economic progress. Variables such as humidity, heat, salinity, metal composition, and others influence corrosion rates. To extend the lifetime of metals, particularly cold rolled steel, researchers are focused on corrosion inhibitors, anodic or cathodic protection, and protective coatings. Due to their ease of application and superior protection behavior, hydrophobic, hybrid materials, and nanocomposites have been employed as protective coatings, which are superior to chromate and phosphate coatings, which are forbidden due to environmental pollution and toxicity (Al-Sodani et al., 2018).

Carbon steels, particularly N80, are widely used in the oil industry. This is primarily due to legitimate worry. However, in the case of the petroleum sector, those steels have insufficient corrosion resistance. Several ways have been proposed to improve their corrosion resistance (Askari et al., 2019). Chemical inhibition is one of the most viable methods for protecting metals and alloys from acidic corrosion utilising organic chemicals or polymers (Lagrenée et al. 2002).

Sulfamic acid-based inorganic acid cleaning is widely used in a wide range of management and technical applications, including multistage flash evaporators (MSF), saltwater desalination facilities, heat exchangers, and

cooling tower systems. Sulfamic acid (amidosulfonic acid),  $\text{H}_2\text{NSO}_3\text{H}$ , is a white translucent solid that is dehydrated, ephemeral, hygroscopic, and deodorized. Many industrialized precipitates dissolve quickly in aqueous sulfamic acid solutions and acquire soluble components (Morad et al., 2008, Ijaola et al., 2020).

When compared to other acids such as sulfuric and hydrochloric acids, sulfamic acid conducts as a potent medium in aqueous solution, although its corroding is significantly less. To prevent metal dissolution during acid cleaning of carbon steel apparatus and pipes, it is necessary to supplement the investigated organic compounds [8]. Organic components, such as benzene rings, N, O, and S heteroatoms (Abdallah et al., 2018, Negm et al., 2007), are known acid obstacles due to the formation of the protective coating that is adsorbed on investigated surfaces.

Some works have recently been carried out for studying prohibition of a steel surface in sulfamic acid medium using several amino acids (Abdel-Fatah et al., 2016), tetra-pyridinium moiety (Obaid et al. 2017), Azo dyes components (Jeyaraj et al., 2005), aquatic root extract of *Salvadora Persica* (Abdel-Fatah et al., 2014), and cationic surfactant (Motamedi et al., 2013). Moreover, several organic inhibitors based on polymers have been reported in potential applications including purification process of natural gases in view of the creation of protecting layer film on the examined surfaces, for orthopedic implantation, and for corrosion resistance (Garcia-Cabezon et al., 2020, Radhamani et al., 2020). (Zachariah and Liu, 2020) incorporated carbon nanotubes (CNTs) to polybenzoxazine (PBz). The prepared composite was characterized using FT-IR, XPS, and TEM. Its effective protection efficiency reached 90.28% for the used polymer, but agglomeration of MWCNTs had a negative effect on the anticorrosion ability. (Kumar and Gasem, 2015) used polyaniline (PANI) to protect steel structure against corrosion. They used EIS to study the anodic and cathodic polarization.

Poly (vinyl chloride-co-vinyl acetate-co-2-hydroxypropyl acrylate) (PVVH) is a flexible polymer characterized by its transparency, sensitivity to fluctuation in temperature, and the capacity to make flexible films with excellent mechanical and structural qualities that may be used in various technical applications (Yassin et al., 2018).

Mechanical strength, hydrophobicity, ionic conductivity, chemical resistance, and thermal properties are some of the many characteristics that set poly(ethyl methacrylate) (PEMA) apart from other synthetic polymers. Many different types of gadgets, from hearing aids to dentures to fossil coating to artificial nails to packaging to medical equipment, all benefit from the PEMA usage as a reliable raw material (Krumenacker, 2019).

Few studies based on PVVH were published in the literature (Yassin et al., 2019, Lei et al., 2011), although PEMA was added into other polymers to study their properties, including poly (vinyl chloride) (Mohan et al., 2011), poly (vinylidene fluoride) (Jayaraman et al., 2016), poly (vinyl acetate) (Premila et al., 2017), and graphene oxide (Mohanty and Swain, 2019).

Different nanofillers (Yassin and Abdelghany, 2021) are generally added to an appropriate polymer in order to improve properties of the final samples in addition to the increment in probability of bring novel properties. Researchers are constantly looking for new and better corrosion-resistant materials that may be used in everyday situations. When two or more polymers are combined, they generate a new material with unique physical and chemical properties that cannot be achieved by using the polymers alone. As a result, this research was carried out in order to develop a highly effective anti-corrosion nanocomposite for use in pipelines during the transit of petroleum products, which will save time and money in the repair of portions affected by corrosion.

PVVH/PEMA, a polymeric blend, and PVVH/PEMA/Au-NPs, a nanocomposite of PVVH/PEMA, were investigated as corrosion inhibitors for N80 steel in 5 % sulfamic acid solutions in this study. The experimental results were verified using electrochemical methods such EIS technique followed by a surface investigation using the SEM technique. We also compared the experimental data with the theoretical quantum chemical parameters obtained using the DFT approach and Mulliken atomic charges.

## 2. Material and methods

### 2.1. 2.1. Materials and reagents

All of the chemicals used came from the Sigma-Aldrich business and were of a high enough analytical chemical grade to be labelled as such. PVVH with molar mass (M.Wt.)  $\approx 33,000 \text{ g.mol}^{-1}$  composed of vinyl chloride with 81 wt%, vinyl acetate with 4 wt%, and 2-hydroxypropyl acrylate with 15 wt%. has Poly (ethyl methacrylate) (PEMA, molecular weight =  $50,000 \text{ g/mol.}$ ) in powder shape. The common solvent used was Tetrahydrofuran (THF) bought from Fisher Scientific (UK).

Electrochemical methods were performed via N80 working electrode of carbon steel sample which has the elemental structure (wt. %): C, 0.026; Mn, 1.51; Si, 0.10; S, 0.02; N, 0.27; Ni, 0.16; Al, 0.35; Cr, 0.27; Cu, 0.28; Nb, 0.93; Ti, 0.11; and the rest Fe.

### 2.2 Synthesis of gold nanoparticles

From gold mass as a precursor, 99.98 percent pure gold nanoparticles (AuNPs) were created using a laser ablation process. Before beginning the ablation procedure with the Nd: YAG nanosecond pulsed laser, the bulk was cleaned and polished before being put in 20 ml of THF.

### 2.3. Synthesis of the polymer blend and its nanocomposite

PVVH and PEMA were each dissolved in 100 ml of THF at their respective weights with the use of a mechanical stirrer. After that, the solutions were combined to make the PVVH/PEMA blend, which was then vigorously stirred for 80 minutes to ensure a consistent final result. PVVH/PEMA/3 wt percent AuNPs was produced by adding AuNPs in predetermined proportions to the already-made combinations. The solutions were placed onto glass Petri plates and baked for 72 hours to remove any remaining solvent. Film thickness for the nanocomposite materials was somewhere around 90 and 120 micrometers.

### 2.4. Measurements

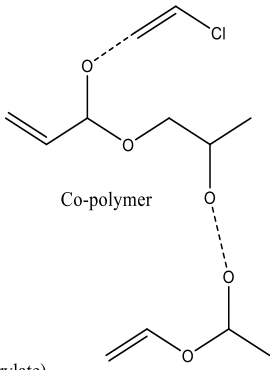
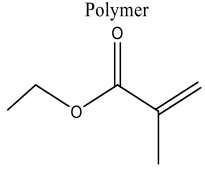
#### 2.4.1. characterization of the blend and its nanocomposite

The polymer blend and the blend/Au-NPs nanocomposite presented in Table 1 were examined as chemical corrosion inhibitors. At 293 K, a high-resolution X-ray diffractometer was used to conduct an X-ray diffraction (XRD) study. Its model is PAN-alytical X'Pert PRO-MRD) with Cu-K $\alpha$  radiation that run at V=30 KV and wavelength = 0.15406 nm). Bragg's angle ( $2\theta$ ) was recorded in the range from 3° to 70°. The materials' structural characteristics in the spectrum region of 4000-550 cm<sup>-1</sup> were studied using a Fourier transforms infrared (FT-IR) spectrometer (Nicolet iS10 single beam). In transmission electron microscopic analysis, the samples were loaded on carbon-coated Cu grids (200 mesh) and examined by HRTEM operated at 200 kV. Its model is JEM-2100, JEOL (Tokyo, Japan).

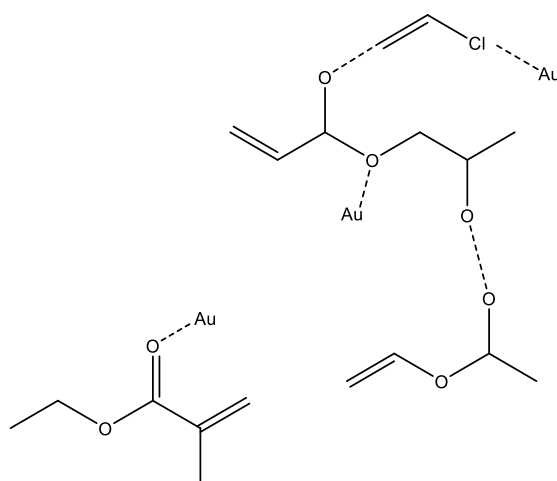
All electrochemical trials were carried out with and without the produced mix polymer and its gold nanoparticles in the corrosive media of 5% sulfamic acid solution. These examined compounds were examined at dosages extending from 5x10<sup>-6</sup> M to 5x10<sup>-4</sup> M. The produced samples were then examined by bead onto the N80 steel surface in a liquid state (i.e., solution). For all surveys, the solutions under deliberation were disposed insolently.

**Table 1**

Names and structures of the investigated polymer blend and its gold nanoparticle compound

Comp.	Structure
<b>I</b>	Poly(vinyl chloride-co-vinyl acetate-co-2-hydroxypropyl acrylate) $[CH_2CH(Cl)]_x[CH_2CH(O_2CCH_3)]_y[CH_2CH[CO_2CH_2CH(OH)CH_3]]_z$
	
Poly(ethyl methacrylate) (PEMA)	
Poly(vinyl chloride-co-vinyl acetate-co-2-hydroxypropyl acrylate)	

## II



PVVH/PEMA/Au nanocomposite

## 2.4.2. Electrochemical measurements

To EIS electrochemical procedures, a Volta lab 80 (Tacussel-Radiometer PGZ402) was used. All electrochemical studies were carried out in a typical 250 mL closed cell, with a 1 cm<sup>2</sup> cross-area working electrode carved from N80 carbon steel. As an auxiliary electrode, a platinum film was erected, and a saturated calomel electrode (SCE) was employed as a reference electrode. Before experiments, the outside surface of the working electrode was scratched with various emery sheets (from 320 to 2000), degreased with propanone (Abdel-Rehim et al., 2006), cleaned with demineralization water, and completely dried. To avoid IR potential descent within either electrode ending, the reference electrode was placed next to the studied steel electrode via a Luggin-Haber capillary.

All trials were directed at 25°C for 30 minutes, with OCP (open circuit potential) being verified until steady state was reached, and all potentials were Vs. SCE.

EIS measurements were achieved using a peak-to-peak AC signal (10 mV) in a potentiostatic method at OCP steady state with frequency varieties of 100 kHz and 30 mHz. All tests were repetitive three times to ensure the accuracy of the results.

The analogous model was used to investigate and interpret all impedance extents. The major variables derived from Nyquist plot analysis are plotted in Fig. 1, which attribute fitting data from EIS plots by the corresponding circuit, where  $R_s$  is the solution resistance,  $R_f$  is the examined inhibitors layer resistance,  $C_f$  is the constant phase element of the inhibitor barrier,  $C_{dl}$  is the constant phase element of the double layer, and  $R_{ct}$  is the charge transfer resistance.

The efficiency of inhibition for the corrosion of N80 steel ( $\eta$  %) in 5% sulfamic acid medium obtained from the polarization resistance  $R_p$  using the subsequent equations (Rosalbino et al., 2011):

$$R_p = R_f + R_{ct} \quad (2)$$

$$\eta \% = \theta \times 100 = \left(1 - \left[\frac{R_p^\circ}{R_p}\right]\right) \times 100 \quad (3)$$

wherever  $R_p^\circ$  and  $R_p$  are the polarization resistance of specimens in 5% sulfamic acid medium without and with polymer blend and its gold nanoparticles compounds, correspondingly.

The impedance  $Z_{CPE}$  can be considered with the subsequent equation:

$$Z_{CPE} = \frac{1}{Y_0(j\omega)^n} \quad (4)$$

wherever  $Y_0$  is the admittance of the CPE,  $\omega$  is the angular frequency ( $\omega=2\pi f$ ), and  $n$  is the CPE index, which is characterized as phase shift.

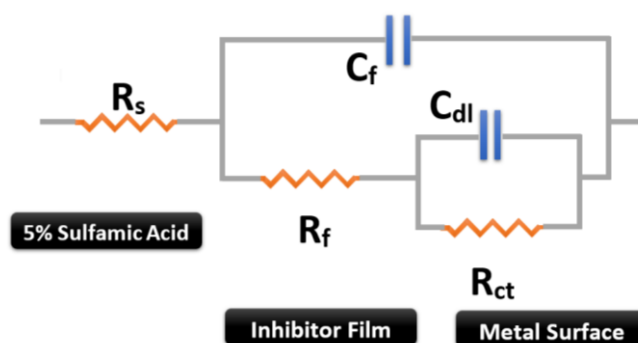


**Figure 1:** The equivalent circuit was used to illustrate electrochemical impedance spectroscopy data with and without various dosage inhibitor concentrations

### 3. Results and Discussion

#### 3.1. Characterization of AuNPs

The transmission electron microscope (TEM) was used to verify the successful production of AuNPs using the laser ablation approach. The TEM micrograph of AuNPs is shown in Fig. 2a, which exhibits the excellent dispersion of Au-NP throughout the solvent. Figure 2b is a TEM micrograph of PVVH/PEMA containing 3 percent Au-NPs. This figure also shows that the Au-NPs are equally dispersed in the polymeric matrix, indicating that the produced nanocomposite's efficacy in improving different attributes is promising. It's also worth noting that the AuNPs had spherical forms with sizes ranging from 3 to 29 nm, indicating that they were successfully synthesized. X-ray diffraction (XRD) was used to investigate the structural features of the AuNPs, with the most distinctive peaks appearing in Fig. 3 at  $38.4^\circ$ ,  $44.94^\circ$ , and  $65.2^\circ$ , respectively, attributed to (111), (200), and (220). Those results are in line with those found on the gold nanoparticle standard card, which is documented in JCPDS File No. 4-0784.

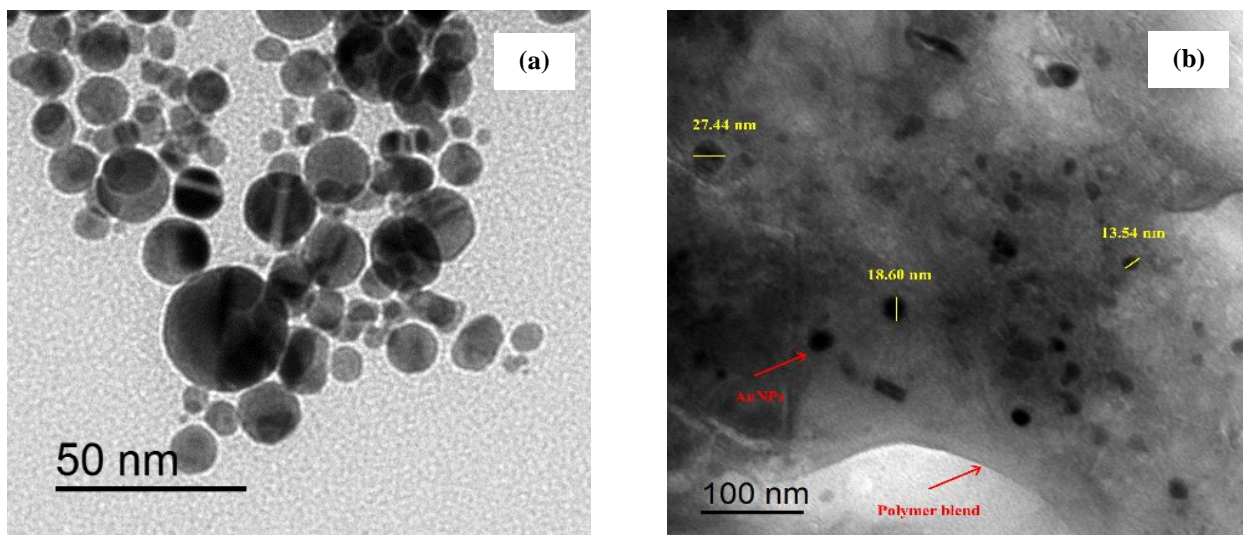


**Figure 2:** TEM micrograph of a) the AuNPs and b) the PVVH/PEMA filled with 3% Au-NPs.

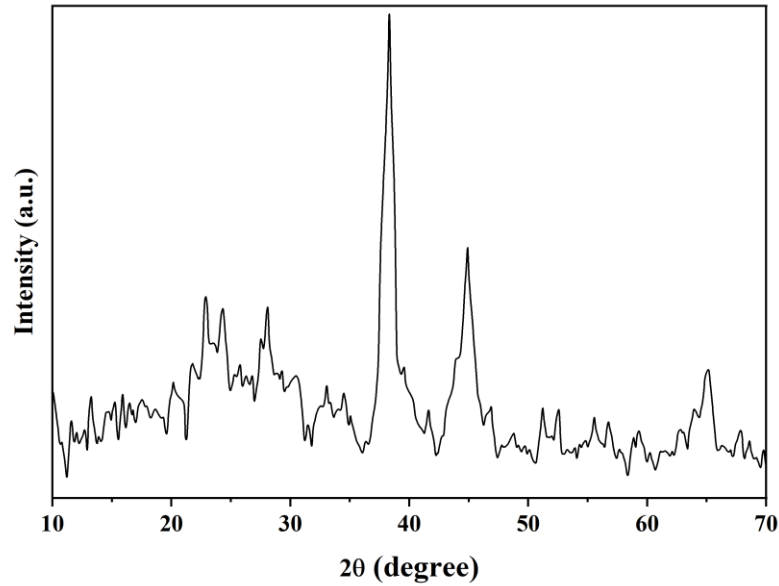


**Figure 3:** XRD representative pattern of the gold nanoparticles.

### 3.2. XRD analysis

Polymer composites' microstructural variations may be better understood with the use of XRD measurements. That's why it was used to verify the amorphous-crystalline nature of the (PVVH/PEMA)/Au nanocomposite films under research, as well as examine how nanocomposite AuNPs affect structural characteristics.

XRD typical patterns of the PVVH/PEMA blend and the blend filled with 3% Au-NPs are given in Fig. 4. The main broad peak observed at  $21.24^\circ$  was ascribed to the PVVH [18], where it has been shifted to  $22.06^\circ$  due to incorporation of PEMA and Au-NPs into the host matrix. Moreover, its broadness demonstrates that the polymer blend and its nanocomposites are semicrystalline. The increase in intensity of this broad peak after adding Au-NPs confirms the compatibility and efficient incorporation of the Au-NPs into the PVVH/PEMA.

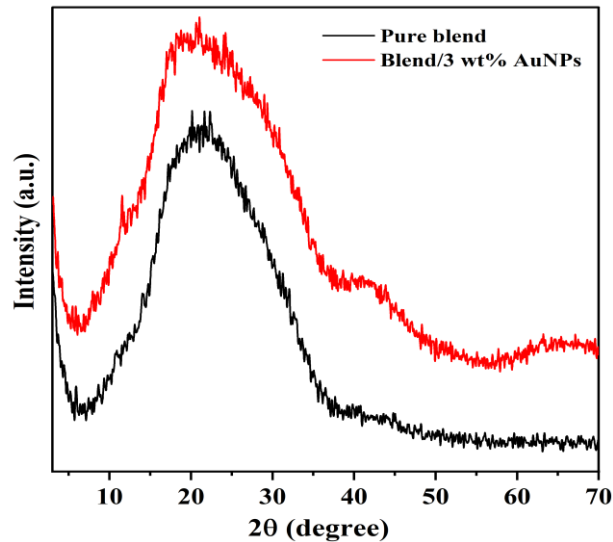


**Figure 4:** XRD representative patterns for the above-described samples.

### 3.3. FT-IR spectroscopic analysis

At 25 °C, spectroscopic analysis based on FT-IR data was utilized to investigate the complexation and intermolecular interaction of PVVH/PEMA with 3 wt % Au-NPs. Figure 5 shows the FT-IR spectra acquired for pure blend and the blend doped with three percentages of AuNPs between 4000 and 400 cm<sup>-1</sup>. Bands at 3621, 1648, 2924, and 774 cm<sup>-1</sup> help to identify the spectra as belonging to PVVH. These bands are ascribed to O-H stretching and bending, symmetrical C-H stretching, and -CH<sub>2</sub> rocking (Kumar and Gasem, 2015).

Besides the 1473 cm<sup>-1</sup> peak associated with PEMA, which was shown to be due to -CH<sub>2</sub> scissoring, two other peaks were seen at 1453 cm<sup>-1</sup> and 1391 cm<sup>-1</sup> due to the existence of asymmetrical -OC<sub>2</sub>H<sub>5</sub> bending and -CH<sub>2</sub> twisting vibrations, respectively (Zain et al., 2020). Additionally, other characteristic peaks in the blend/ 3% AuNPs spectra and their assignment were summarized in Table 2.

The presence of oxygen in the ether linkage affords a favorable environment for the formation of intermolecular hydrogen bonds with various molecules in the PEMA polymer, as evidenced by the observed modification in the intensities of some peaks and the formation of hydrogen bonds, proving the exact interaction arose in the polymer matrix (Elashmawi, et al., 2014).

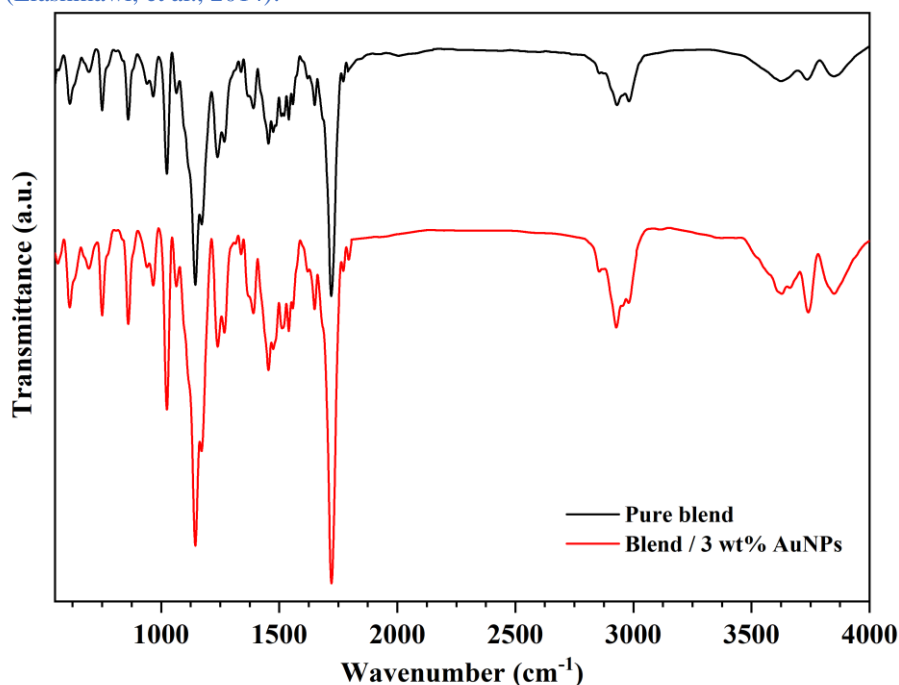


Figure 5: FT-IR spectra of the pure blend and the blend filled with 3 wt% of AuNPs.

Table 2

Bands' Assignment for the FT-IR spectra of PVVH/PEMA samples under study

Wavenumber (cm <sup>-1</sup> )	Band assignment
3621	O-H stretching
2983	asymmetrical C-H stretching
2924	symmetrical C-H stretching
2855	symmetrical C-H stretching
1717	C=O stretching
1648	O-H bending
1473	CH <sub>2</sub> scissoring
1453	asymmetrical -OC <sub>2</sub> H <sub>5</sub> bending
1391	CH <sub>2</sub> twisting
1367	CH <sub>2</sub> bending

1337	O–H bending
1239	C–OH stretching
1170	C–O–C stretching
965	out-of-plane rings C–H bending
774	CH <sub>2</sub> rocking
749	asymmetrical -C-C-O bending
694	C–Cl stretching
610	–CH wagging

### 3.4. Potentiodynamic polarization (pp)

Tafel polarization plots are commonly established to give suitable statistics with the kinetics of electrochemical corrosion variables. The PP sketches of N80 carbon steel in 5% sulfamic acidic solution, including different portions of PVVH/PEMA blend filled with 3% Au-NPs at room temperature are illustrated in Fig. 6 (A-B) at 25°C and Fig. 7 (A-B) at 55°C.

The PP curves demonstrate that the examined inhibitors diminish corrosion of N80 surface compared to the unprocessed samples. This finding was concluded through the anodic and cathodic Tafel plots that exhibited a reduction in corrosion rates. The PP technique parameters as corrosion potential ( $E_{corr}$ ), Tafel slopes ( $\beta_a$ ,  $\beta_c$ ), corrosion current density ( $i_{corr}$ ) and corrosion inhibition efficiency ( $\eta$  %) were evaluated by motivating anodic and cathodic Tafel plots as reported in Table 3.

The decrease in the  $i_{corr}$  values with increasing the concentration of examined polymeric samples was attributable to constant polymer adsorption at the electrode/medium interact. This behavior has impeded active sites, and proscribed their interact with corroding ions in examined acidic medium. So, metal dissolution reduces and also, ( $i_{corr}$ ) reduced. Furthermore, it is noted that Tafel slopes ( $\beta_a$ ,  $\beta_c$ ) aren't altered significantly with adding examined polymer blend with various concentrations. This stated that by adding synthesized blend polymer and nano-formation to 5% sulfamic acid as corrosive media does not change the reaction mechanism however inhibits its rate and delaying the anodic metal dissolution, and cathodic oxygen reduction reactions (Shalabi et al., 2014). Therefore, the arrange of increasing inhibition efficiency ( $\eta$  %) is as follows: Blend/ 3% Au-NPs > Polymer blend, correspondingly. (Liu et al., 2021) reported that the value of  $\eta$  % reached 76.1 % by using the potentio-dynamic polarization measurements, and (Hsissou et al., 2020) found that the best value for their polymer-based inhibitor was 89.55%, whereas  $\eta$ % of the present nanocomposite attained 91.3% at room temperature. This gives our nanocomposite comparative advantages over the other composites.

The corrosion inhibition could be assigned to the adsorption of synthesized nanocomposite constituents on the examined surface. This occurs through lone two of electrons on the oxygen atoms and empty d-orbital of examined interface with donor-acceptor responses. Consequently, a protective barrier is molded, which could increase the inhibition tendency for corrosion.

**Table 3**

Electrochemical kinetic variables of the Tafel diagrams for carbon steel occupied in 5% Sulfamic acid in presence or absence of differing concentrations of examined blend polymer and its Au nanoparticles at 25°C and 55°C correspondingly

Temp.	Inhibitor	Conc., (M)	$-E_{corr.}$ mV(vs. SCE)	$i_{corr.}$ , $\mu\text{Acm}^{-2}$	$\beta_a$ , $\text{mVdec}^{-1}$	$\beta_c$ , $\text{mVdec}^{-1}$	$\theta$	$\eta$ %
25°	Blank	----	526.4	352.7	86.4	-145.2	----	-----
	Polymer blend	5x10 <sup>-6</sup>	507.3	209.3	77.7	-191.4	0.407	<b>40.7</b>
		1x10 <sup>-5</sup>	543.1	168.1	85.4	-157.5	0.523	<b>52.3</b>
		5x10 <sup>-5</sup>	531.5	135.2	72.8	-179.1	0.617	<b>61.7</b>
		1x10 <sup>-4</sup>	552.4	87.4	91.3	-190.1	0.752	<b>75.2</b>
		5x10 <sup>-4</sup>	518.2	42.1	80.2	-204.6	0.881	<b>88.1</b>
		5x10 <sup>-6</sup>	543.1	191.3	111.5	-159.7	0.458	<b>45.8</b>



	<b>Blend/ 3%</b> <b>Au-NPs</b>	1x10 <sup>-5</sup>	491.2	149.6	127.1	-157.3	0.576	<b>57.6</b>
		5x10 <sup>-5</sup>	512.7	112.1	128.4	-156.6	0.682	<b>68.2</b>
		1x10 <sup>-4</sup>	534.6	73.2	118.8	-142.2	0.792	<b>79.2</b>
		5x10 <sup>-4</sup>	521.3	30.8	123.8	-137.0	0.913	<b>91.3</b>
<b>55°C</b>	<b>Blank</b>	----	531.5	1269.4	93.1	-163.2	----	----
	<b>Polymer blend</b>	5x10 <sup>-6</sup>	543.2	871.2	126.7	-189.3	0.3137	<b>31.4</b>
		1x10 <sup>-5</sup>	520.1	712.5	91.6	-173.9	0.4387	<b>43.9</b>
		5x10 <sup>-5</sup>	512.3	598.7	130.1	-155.7	0.5284	<b>52.8</b>
		1x10 <sup>-4</sup>	536.8	486.1	135.4	-176.2	0.6171	<b>61.7</b>
		5x10 <sup>-4</sup>	548.1	264.3	109.5	-147.6	0.7918	<b>79.2</b>
	<b>Blend/ 3%</b> <b>Au-NPs</b>	5x10 <sup>-6</sup>	524.3	781.1	123.7	-166.2	0.3847	<b>38.5</b>
		1x10 <sup>-5</sup>	548.1	638.3	149.1	-196.6	0.4972	<b>49.7</b>
		5x10 <sup>-5</sup>	563.4	529.7	146.2	-207.3	0.5827	<b>58.3</b>
		1x10 <sup>-4</sup>	511.9	373.5	91.3	-208.7	0.7058	<b>70.6</b>
		5x10 <sup>-4</sup>	<b>536.7</b>	<b>191.4</b>	<b>139.8</b>	<b>-214.3</b>	<b>0.8492</b>	<b>84.9</b>

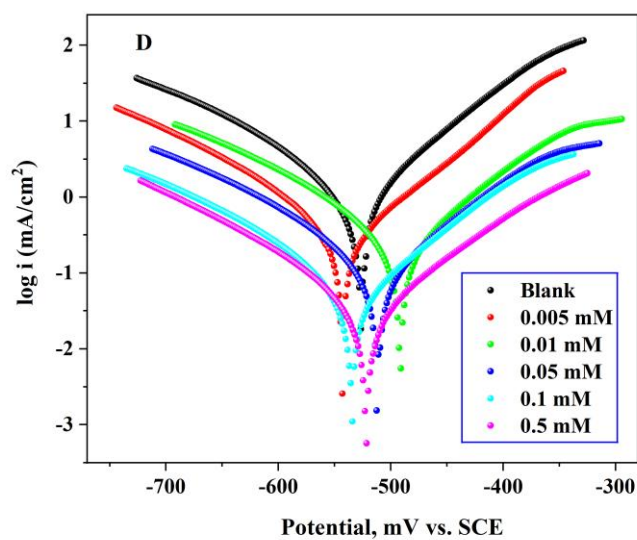
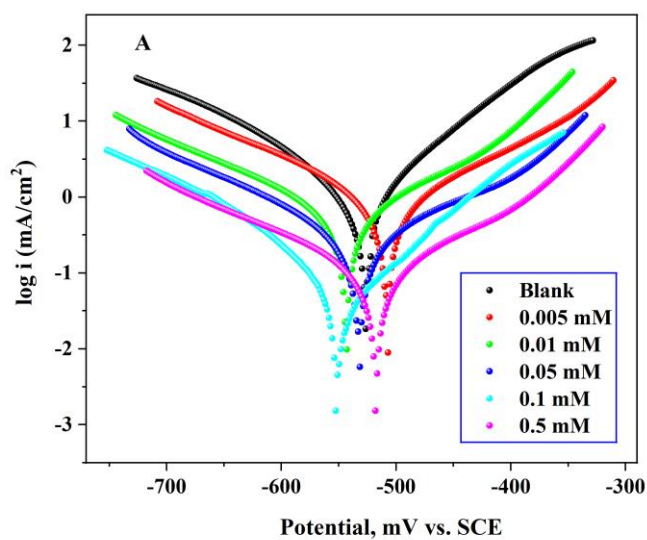


**Figure 6:** Tafel diagrams for N80 carbon steel with and without of (A) Polymer blend, (B) Blend/ 3% Au-NPs, in 5% sulfamic acid at 25 °C.

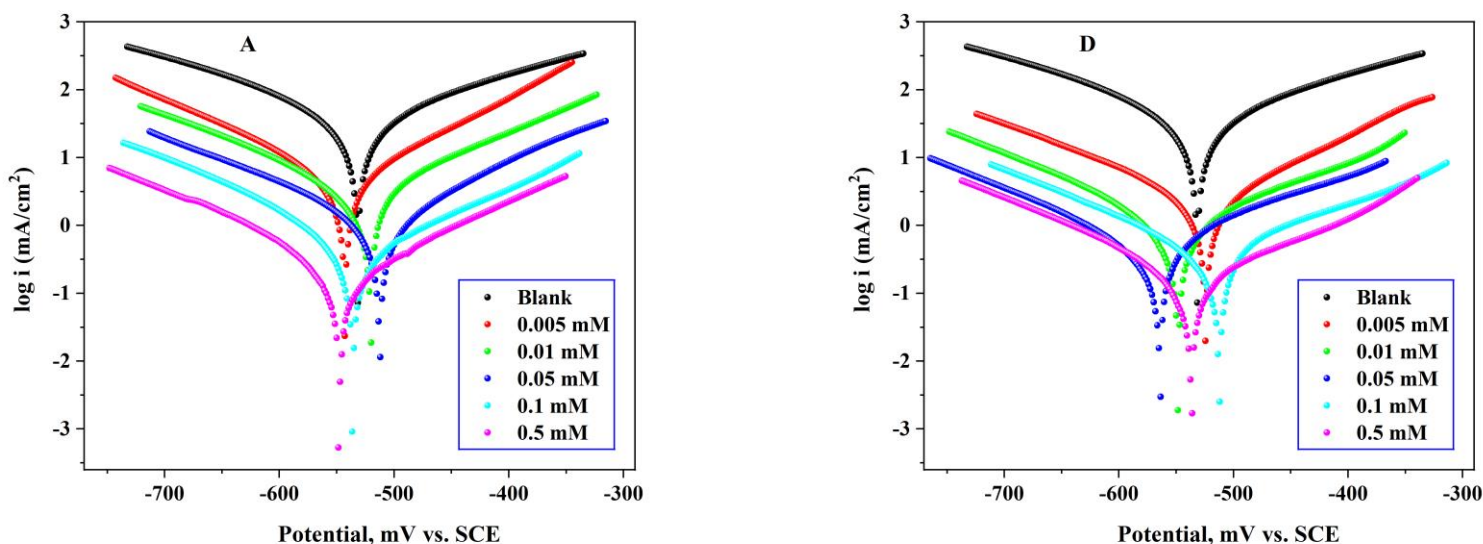


**Figure 7:** Tafel diagrams for N80 carbon steel with and without of (A) Polymer blend, (B) Blend/ 3% Au-NPs, in 5% sulfamic acid at 55°C.

### 3.5. EIS measurements

Because of its suitability for studying corrosion at the metal/electrolyte interface, electrochemical impedance spectroscopy was used. Figures 8a-b and 9a-b show Nyquist and Bode designs of N80 carbon steel in a corrosive media containing 5% sulfamic acid, with and without different doses of investigated polymer mix and gold nano production. The diameter of bends determines the charge transfer resistance  $R_{ct}$ , hence the  $R_{ct}$  values of N80 carbon steel in a 5% sulfamic acid media are unrelated to the investigated manufactured polymers (viz., The diameter of semicircles raises).

All of the capacitive loops showed defective semicircles with the center under the X-axis as concentrations of the tested inhibitors were increased to the corrosive medium of 5% sulfamic acid. This was caused by frequency dispersion caused by the adsorption of the PVVH/PEMA blend and its nanocomposite onto the investigated steel contact, resulting in a heterogeneous electrode interface (Deng and Xie, 2014). The radii of semicircle capacitive loops were increased by increasing the concentrations of the tested materials, as shown in Fig. 8 a-b. That altitude is mentioned in charge transfer resistance ( $R_{ct}$ ) without changing the corrosion reaction mechanism. Furthermore, the phase angle plots for the investigated inhibitors in (Fig. 9 a-b) showed that when the Au-NP concentrations increased, the phase angle plots became broader. These factors suggest the suppression of N80 carbon steel corrosion in a 5% sulfamic acid solution by these polymeric samples (Mert et al., 2014). The EIS technique parameters were quantitatively investigated using Zsimpwin V3.06 software to match the electrical equivalent circuit, as shown in Fig. 1, and the fitted values are listed in Table 4. Figure 1 shows the proper matching circuit for fitting EIS data which collected of solution resistance ( $R_s$ ), film resistance ( $R_f$ ), film constant phase element ( $CPE_f$ ), constant phase element for double layer ( $CPE_{dl}$ ) and charge transfer resistance ( $R_{ct}$ ). The impedance of the CPE ( $Z_{CPE}$ ) might be described as in equation (4).

The values of  $n$  factor changed in the range of 0.931-0.998 ( $0 < n < 1$ ) signifying the insufficient capacitive approach that ascribed to the inhomogeneous of exterior roughness, surface dissolution, diffusive of effective centers, and the mechanism of adsorption of the studied samples on the N80 carbon steel interface as observed in **Table 4** (Oguzie et al., 2004).

When the blend polymer and gold nanoparticles are adsorbed on the steel contact, anodic dissolution happens only in the surface area, resulting in extremely uneven current dispensation (Dehghani et al., 2020). As demonstrated in Table 4, the  $R_s$  values fall as the inhibitor concentration increases, encouraging the adsorption of the tested polymers on the steel interface and increasing the double layer diameter. Although the  $R_{ct}$  values fell as the concentrations of the tested polymers increased, this suggests that the adsorption of these polymers on the steel contact provided a protective barrier against the corrosive 5 % sulfamic acid solution. The experimental evidence verifies that inhibition efficiency (IE %) of the examined polymers at various concentrations expansions as the following sequence: Polymer blend/ 3% Au-NPs > blend Polymer, correspondingly, confirming the PP conclusions.

**Table 4**

Electrochemical variables acquired from EIS equivalent circuit appropriate of carbon steel included to 5% Sulfamic acid without and with various doses of inhibitors.

Inhibitors	Conc. of inhibitor (M)	$R_s$ , ( $\Omega \text{ cm}^2$ )	$n$	$C_{dl}$ , ( $\mu\text{F}/\text{cm}^2$ )	$R_{ct}$ , ( $\Omega \text{ cm}^2$ )	$\eta$ %
blank	----	1.367	0.996	418.3	170.5	----
Polymer blend	$5 \times 10^{-6}$	2.306	0.986	271.9	272.3	37.4
	$1 \times 10^{-5}$	1.681	0.964	219.4	350.2	51.3
	$5 \times 10^{-5}$	1.376	0.931	167.5	423.1	59.7
	$1 \times 10^{-4}$	2.274	0.966	143.7	591.8	71.2
	$5 \times 10^{-4}$	2.437	0.985	85.9	1207.4	85.9
Blend/ 3% Au-NPs	$5 \times 10^{-6}$	1.192	0.995	234.1	308.6	44.8
	$1 \times 10^{-5}$	1.541	0.948	173.9	389.3	56.2
	$5 \times 10^{-5}$	1.465	0.977	148.6	493.7	65.5
	$1 \times 10^{-4}$	1.905	0.993	108.4	789.8	78.4
	$5 \times 10^{-4}$	1.381	0.998	62.1	1547.2	89.0

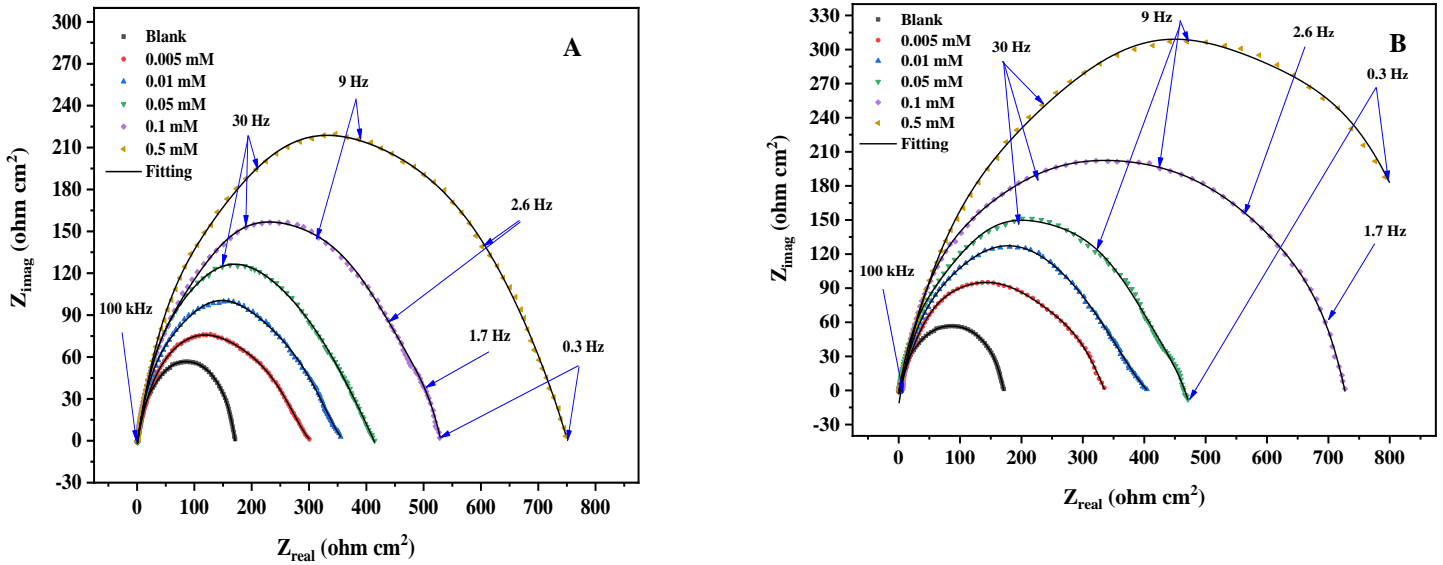


**Figure 8:** Nyquist diagrams for N80 carbon steel with and free of (A) Polymer blend, (B) Blend/ 3% Au-NPs, in 5% sulfamic acid at 25 °C

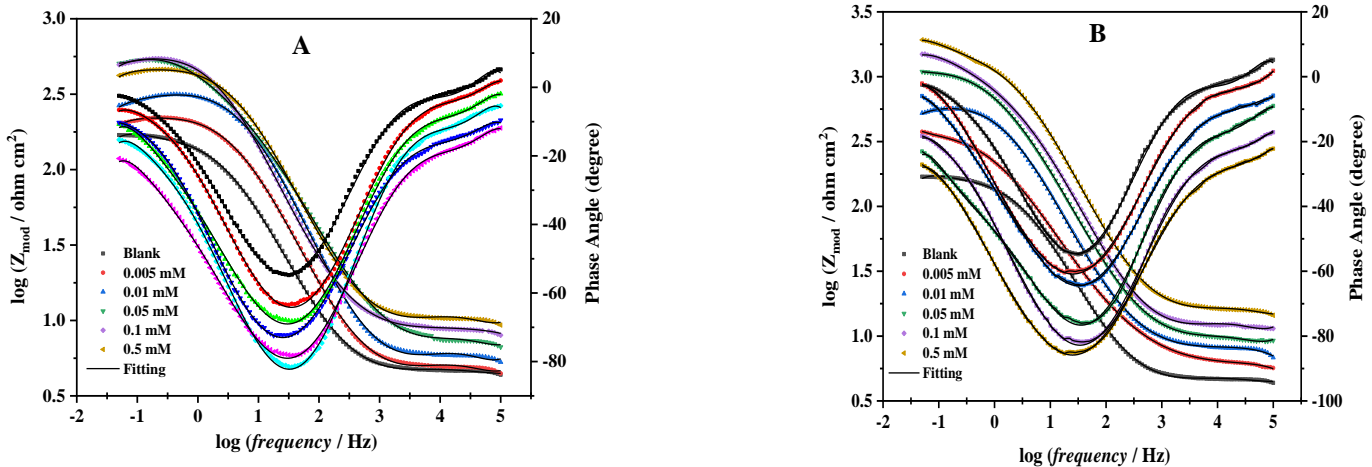


**Figure 9:** Bode plots for N80 carbon steel with and free of (A) Blend polymer and (B) Blend Polymer/ 3% Au, in 5% sulfamic acid at 25 °C

3.6. Surface morphology (SEM, Scanning electron microscope examination):

SEM morphology was used to analyse the adsorption of the investigated mix polymer and its Au nanoparticles with varied compositions on the carbon steel surface. The results of morphology analysis of carbon steel surface tested by SEM prior to and after adding 5% sulfamic acid medium with and without the maximum concentration of tested blend polymer and its Nano compounds ( $5 \times 10^{-4}$  M of blend polymer and blend polymer with 3% Au-NPs) for 24 hours a day are shown in Fig. 10 A–D. The scanning electron microscope micrographs of tested carbon steel specimens only in the absence of either additive (Free steel Fig. 10A), (specimen B) reveal that carbon steel specimens processed with 5% sulfamic acid medium have corroded regions on the refined exterior that

do not appear on the free specimen. The existence of these regions would be admitted to the iron dissolution as a result of the surface attack by the forceful sulfamic acid.

Preoccupation of the tested steel specimens in 5% sulfamic acid medium, including the examined blend polymer (specimen C) and blend polymer with 3% Au (specimen D), revealed that the morphology of steel is strengthened as a result of reducing corroding regions as a result of wrapping active sites in investigated inhibitors. This process entails exposing the outside via a protective layer, resulting in a more homogeneous surface. This means that the corrosion rate is lower in the presence of all examined polymers than in corrosive environments without inhibitors.

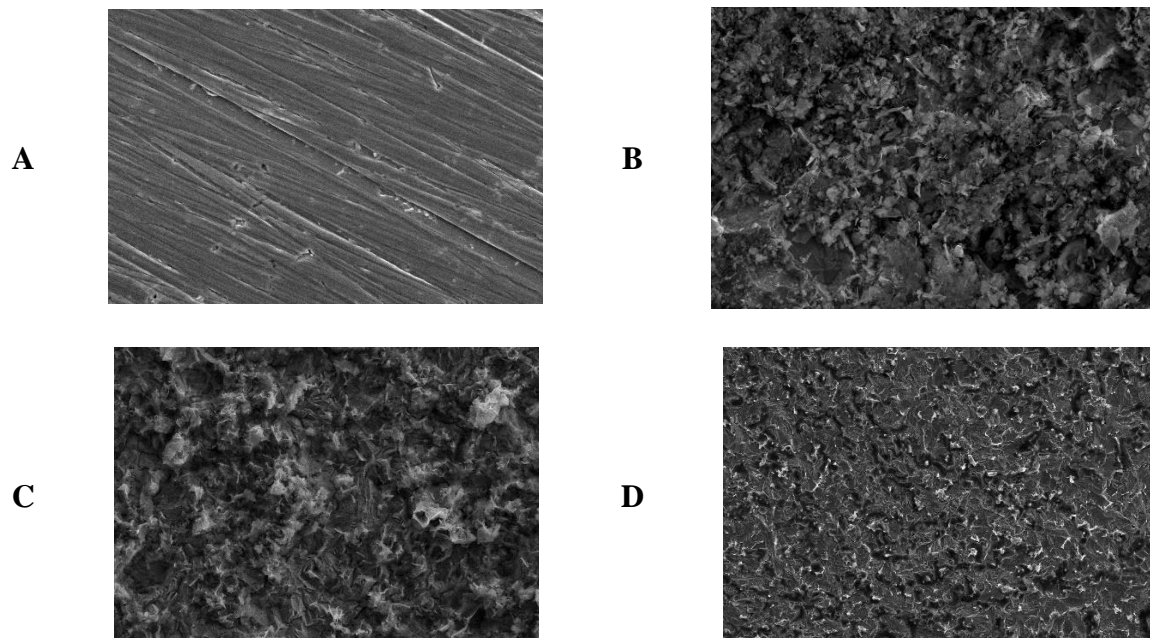


**Figure 10:** SEM micrographs of carbon steel prior and after engaged in 5% sulfamic acid solutions with optimum contents of tested polymers: (A) steel without any additives (Free steel) (B) after 24 hours ducking in 5% M sulfamic acid medium (C) after 24 hours ducking in 5% M sulfamic acid involving  $5 \times 10^{-4}$  M of blend polymer (D) after 24 h ducking in 5% M sulfamic acid involving  $5 \times 10^{-4}$  M of the polymer blend with 3% AuNPs at 25 °C.

### 3.7. Quantum chemical parameters of protonated polymers (DFT studies and Mulliken atomic charges)

$E_{\text{HOMO}}$  suggests the susceptibility of the studied steel to provide electrons to the acquired recipient with empty molecular orbitals, while  $E_{\text{LUMO}}$  suggests the susceptibility to receive these electrons. The small assess of  $E_{\text{LUMO}}$ , the further susceptibility to receive electrons (Gao and Liang, 2007).

The greater assess of  $E_{\text{HOMO}}$  of the investigated blend polymers, the better its capability to provide electrons to the empty  $d$ -orbital of carbon steel exterior, and the better its efficiency of inhibition. The calculated values scheduled in **Table 5** display that the greatest energy  $E_{\text{HOMO}}$  is appointed for the tested components, where blend polymer / 3% Au nanoparticles (-4.09 eV) is supposed to have the better corrosion inhibition amongst the tested inhibitors. The existence of hydroxy group destabilizing the HOMO smooth which is best noted in case of blend polymer/ 3% Au nanoparticles.

Thus, it has highest propensity to adsorption on carbon steel exterior also it has the best inhibition tendency. These agrees with all experimental methods proposing the highest inhibition efficiency for the blend polymer/ 3% Au nanoparticles.

Thus, it has the best ability to adsorb on the carbon steel exterior and therefore has the best inhibition efficiency. This agrees with all experimental techniques data which indicates the best inhibition efficiency for the blend/ 3% Au nanoparticles. As listed in **Table 5** and noted such the differentiation in LUMO energies values between the investigated polymers is dominate lower, and also inhibition efficacy is irrelevant to modifications of the  $E_{LUMO}$  values.

$E_{HOMO} - E_{LUMO}$  energy gap,  $\Delta E$  approximate, that is a major stability index, is utilized to formulate hypothetical models to describing structure and configuration of shields in various molecular systems. The smaller value of  $\Delta E$ , the further is the presumed inhibition efficacy of the investigated polymer has (Shalabi et al., 2015). The dipole moment  $\mu$  parameter, electric field, was accustomed to consider and confirm the formulation and the structure of protective films on tested surface (Ozcan et al., 2004). It was demonstrated upon **Table 5** that blend polymer/ 3% Au nanoparticles molecule has the minimal  $\Delta E$  comparison with the alternative inhibitors. Hence, it might be supposed that blend polymer/ 3% Au nanoparticles inhibitor has further tendency to adsorb on carbon steel exterior compared with other tested polymers. The greater values of  $\mu$ , the more is the expected inhibition efficacy the inhibitor has. The computations demonstrated that the greater value of  $\mu$  is appointed for blend polymer/ 3% Au nanoparticles molecule which has the greatest inhibition efficiency.

There exists a common accord by various researchers that the more negatively indicted hetero atoms (-O, -S or -N) is, the better is its capability to adsorb on carbon steel specimen during a donor-acceptor kind reaction (Li et al., 2007).

Small amounts of electronegativity ( $\chi$ ) furthermore provide good potential susceptibility for the tested polymers molecules to yield electrons to examined steel face, so blend polymer has a lower value of  $\chi$  (2.99) than gold nanoparticles (3.31), indicating the high adsorption for the polymer blend which dissimilar with the recent data and results, and this could be as a result of elevated steric hindrance to the blend polymer compound, and reduces its adsorption on the carbon steel (Palaniappan et al., 2020). Moreover, the stability and receptiveness of the molecule can evaluate from hardness ( $\beta$ ) and softness ( $\sigma$ ), i.e., soft polymers have further protective capability than hard polymers due to integrity of the easy electrons' distribution to the examined steel within adsorption process; thus, they are reviewed as efficient corrosion inhibitors (Obot et al., 2015).

**Table 5**

The considered quantum chemical variables for the polymer blend and blend/ 3% Au nanocomposite.

	Polymer blend	Blend/ 3% Au-NPs
$E_{HOMO}$ , eV	-5.13	-4.09
$E_{LUMO}$ , eV	-0.85	-2.52
$\Delta E$ , eV	4.28	1.57
<b>I</b>	5.13	4.09
<b>A</b>	0.85	2.52

$\chi$	2.99	3.31
$\beta$	2.14	0.78
$\sigma$	0.47	1.28
$\Delta N$	0.94	2.36
<b>Dipole moment, <math>\mu</math> debye</b>	3.12	3.69
<b>Molecular surface area, <math>\text{\AA}^2</math></b>	475.75	483.10

As demonstrated in **Table 6**, PVVH/PEMA/ 3% Au-NPs molecule keeps to have less ( $\beta$ ) standards and greater ( $\sigma$ ) values than blend polymer, this such obviously suggests the excellent inhibitor accomplishment to donate electrons to steel surface then higher inhibition potency.

$\Delta N$  values demonstrate the tendency of the compound in providing the tested exterior by electrons. The greater the  $\Delta N$  value, the greater tendency of tested polymers to supply with electrons (Lukovits et al., 2001). According to the estimation rates of  $\Delta N$  which registered in **Table 6**, blend/ 3% Au nanoparticles molecule (2.36) has higher  $\Delta N$  value than blend polymer (0.94). This implies that the blend/ 3% Au-NPs nanocomposite has excellent feature to provide electrons to the steel surface than polymer blend, recommending it for potential applications.

In addition, the inclination of the tested polymers to protect the examined carbon steel in corroding medium is associated to its surface area. The potency of inhibition increments as the extent of the molecular structure increments as the interact area within the examined inhibitor compounds and the carbon steel exterior increases. As appointed in **Table 5**, the nanocomposite filled with 3% Au shows the highest molecular surface area, considering the greater inhibition efficiency for the blend/ 3% Au nanocomposite ( $483.10 \text{ \AA}^2$ ) than the polymer blend ( $475.75 \text{ \AA}^2$ ).

Alteration in the potency of inhibition of tested compounds relies to existence of electronegative (O-) atoms in their molecular structure as provided in **Fig. 11**.

Moreover, molecular electrostatic potential mapping (MEP) could explore the active centers of examined polymers compounds and be figured to utilize the Dmol3 module. The MEP mapping is a 3D graphical form intended to recognize the profit electrostatic persuade based on a molecule by total charge exemption (Madkour et al., 2018). As stated by the MEP maps displayed in **Fig. 12**, the red ensign delineates maximum electron density area whereas the MEP is maximum negative (nucleophilic reaction). In diversity, the blue ensign explains the highest positive area (electrophilic reaction) (Gece and Bilgiç, 2009).

Contrarily, MEP showed the maximum likely positive region over hydrogen atoms in examined compounds. These active centers with extreme electron density (i.e., red centers) in polymer compounds might be the suitable for synergies through carbon steel, building extremely adsorbed protecting barrier.

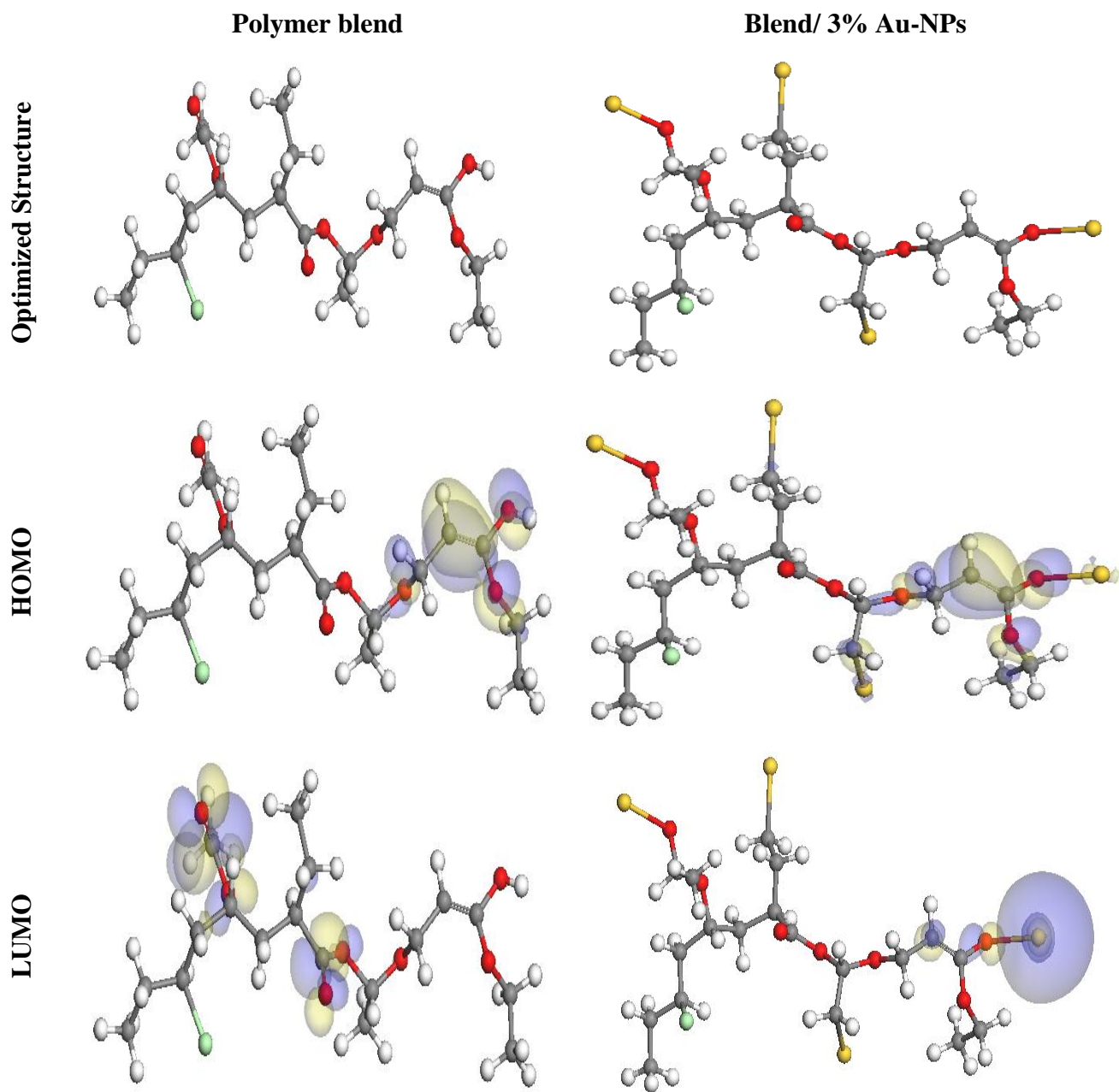


**Figure 11:** The optimized molecular structures, LUMO and HOMO, of the blend polymer and blend polymer/ 3% Au nanoparticles using DMol3 module.



## Molecular Electrostatic Potential (MEP)

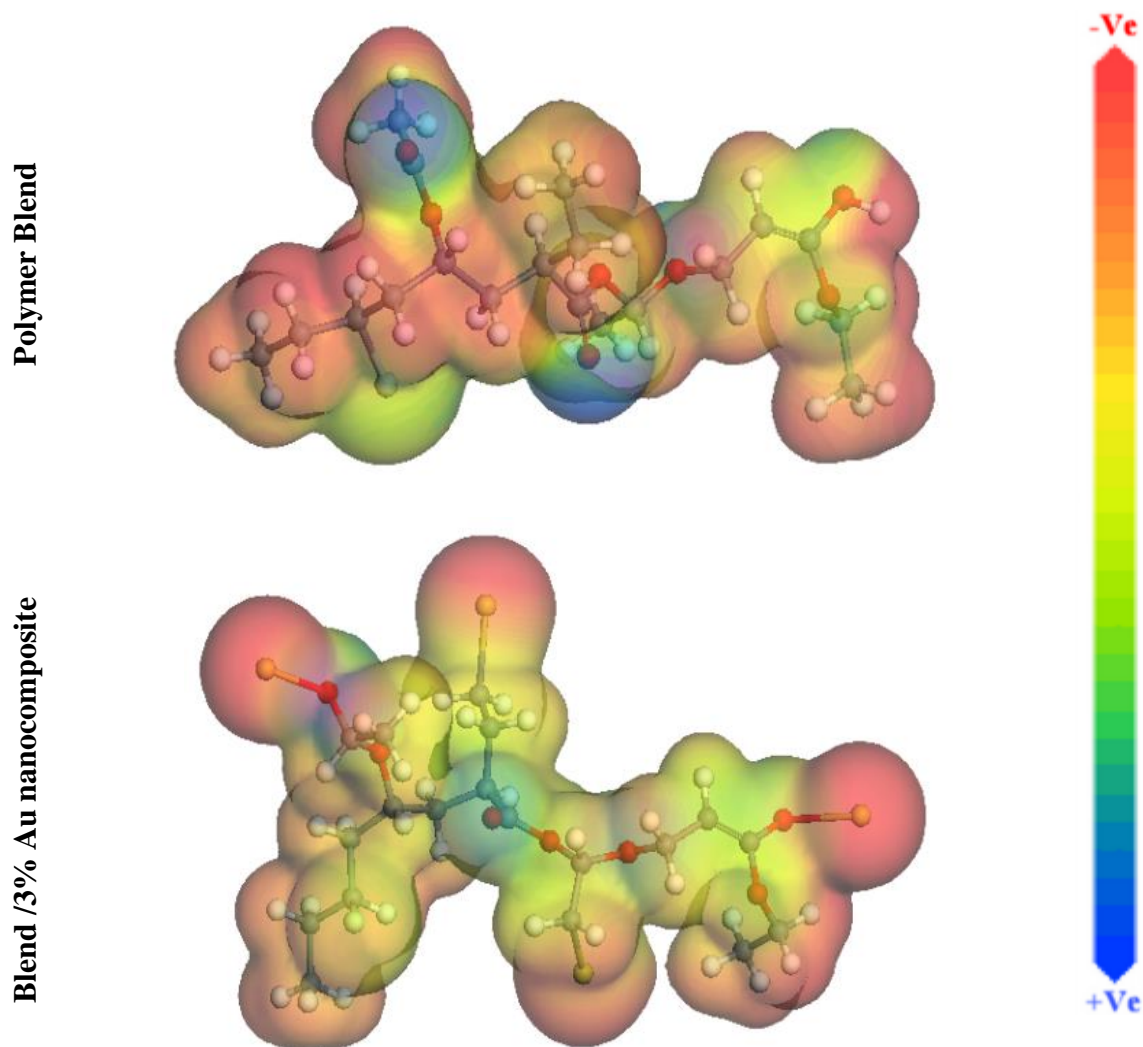


**Figure 12:** Graphical map of MEP of the blend polymer and blend polymer/3 % Au nanoparticles using DMol3 module.

The atomic Mulliken charge is additional signifier that decides the local receptiveness of a compound. The atomic charges of the examined blend polymers and its Au nanoparticles are described in **Table 6**. The atoms hold greater negative charges (red color) are behaved as electron providers (nucleophilic sites). Accordingly, the atoms O3, O4, Cl8, C14, O20, C22, O24 and O27 of blend Polymer and moreover the atoms O3, O4, Cl8, C14, O20, C22, O24 and O27 of blend polymer/ 3% Au nanoparticles are intended as effective spots accomplished to donating electrons to the examined steel surface.

**Table 6**

Calculated Mulliken atomic charges for blend polymer and blend polymer/ 3 % Au nanoparticles

<b>Polymer Blend</b>	<b>Mulliken atomic charges</b>	<b>Blend/ 3% Au-NPs</b>	<b>Mulliken atomic charges</b>
<b>C (1)</b>	0.577	C (1)	0.484
<b>C (2)</b>	-0.167	C (2)	-0.141
<b>O (3)</b>	-0.485	O (3)	-0.751
<b>O (4)</b>	-0.489	O (4)	-0.581
<b>C (5)</b>	0.218	C (5)	0.224
<b>C (6)</b>	-0.073	C (6)	-0.076
<b>C (7)</b>	0.077	C (7)	0.066
<b>Cl (8)</b>	-0.260	Cl (8)	-0.280
<b>C (9)</b>	-0.014	C (9)	-0.038
<b>C (10)</b>	-0.100	C (10)	-0.120
<b>C (11)</b>	-0.030	C (11)	-0.070
<b>C (12)</b>	-0.099	C (12)	-0.087
<b>C (13)</b>	-0.046	C (13)	-0.038
<b>C (14)</b>	-0.104	C (14)	-0.282
<b>C (15)</b>	0.571	C (15)	0.559
<b>O (16)</b>	-0.495	O (16)	-0.496
<b>O (17)</b>	-0.494	O (17)	-0.486
<b>C (18)</b>	0.467	C (18)	0.506
<b>C (19)</b>	-0.104	C (19)	-0.344
<b>O (20)</b>	-0.538	O (20)	-0.561
<b>C (21)</b>	0.186	C (21)	0.172
<b>C (22)</b>	-0.161	C (22)	-0.206
<b>C (23)</b>	0.598	C (23)	0.573
<b>O (24)</b>	-0.554	O (24)	-0.575
<b>C (25)</b>	0.209	C (25)	0.199
<b>C (26)</b>	-0.097	C (26)	-0.124
<b>O (27)</b>	-0.501	O (27)	-0.648
		Au (28)	0.602
		Au (29)	0.617
		Au (30)	0.368
		Au (31)	0.310

### 3.8. Mechanism of inhibition

The corrosion inhibition of tested blend polymer and its 3% nanoparticles in the corrosive media of 5% sulfamic acid in the existence and lack of the examined polymers at 25°C as presented by EIS were expected to depend on the concentrations and the composition of the tested polymers. Hence, in our paper, it has been exhibited that there is a linked covalent bond between nanoparticles and conducting polymer, controlling to significant advance in the corrosion protecting. This takes place in diverse paths, as avoiding the approach of corroding ions to the surface by virtue of the nano-particles size of the examined polymers. Furthermore, the modifications caused in the inhibition effect of the examined blend polymer and the increasing in the exposure surface of examined polymer

are two appropriate causes. All of those factors give rise to enhance achievement than without compounds polymers examined as corrosion inhibitors.

Frequently, it is evaluated that the mechanism of adsorption of the tested inhibitors at the carbon steel interface is the main stage in the corrosion mechanism of the studied polymers in 5% sulfamic acid solutions. In aqueous acidic solutions, the studied particles retaining N, S or O atoms be additionally as neutral atoms or in protonated form (Prabhu et al., 2008).

Four actions of adsorption could take place within corrosion inhibition regarding these studied components on the tested carbon steel surface (Abdallah and Shalabi, 2015):

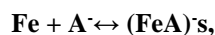
- A. Electrostatic attractiveness forces within the examined carbon steel and protonated ions of the examined polymers.
- B. communication of singular unpaired  $e^-$  of the studied inhibitors with the carbon steel surface;
- C. contact of  $\pi$ -electrons of the studied polymers and carbon steel surface;
- D. Association of all of these processes.

The inhibition productivity is qualified on several causes as; number of adsorption locations and its charge density, molecular weight (M. Wt) of the studied polymers and construct of interrelation with the carbon steel surface (Abdallah et al., 2020).

Likewise, it is genuine that adsorption of the tested polymers on N80 carbon steel exterior could instantly occur in terms on of donor-acceptor accomplishment within the lone pair of hetero-atom (N, O or S) and the widely delocalized electrons of examined polymers and vacant  $d$ -orbital of the carbon steel which is chemisorption adsorption (Ahamad and Quraishi, 2010).

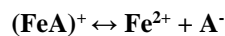
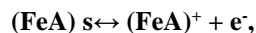
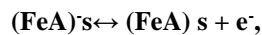
#### **Anodic direction reaction:**

A surface complex is created in the anodic direction reaction and then the complex is desorbed from the iron surface as reported to the following:



#### **Cathodic direction reaction:**

Corrosion mechanism of cs metal in 5% sulfamic acid solutions, in case of  $\text{H}_2\text{NSO}_3^-$  ion, its adsorption on the anodic sites is equivalent as a result to the high electron density (the negative charge and the lone pair of electrons of N atom). Adsorption of sulfamate ions causes high surface coverage or the obtained surface complex is stable to prevent the cs surface from corrosion and so obtaining increase to low corrosion rate.



where  $\text{A}^-$  is  $\text{H}_2\text{NSO}_3^-$  ions and s represents ions or nanoparticles at the surface.

#### **Conclusion**

In the current study, we used a solution casting approach to effectively prepare a polymer blend of PVVH and PEMA filled with Au-NPs, with the Au-NPs themselves being generated using a laser ablation process. XRD, TEM, and FT-IR spectroscopic investigations confirmed the semicrystalline nature of the PVVH/PEMA mix and its nanocomposite. They were also examined as corroding inhibitors for N80 carbon steel in 5% sulfamic acid solutions by electrochemical techniques: PP and EIS which exposed that these inhibitors are active and confirmed that the examined polymer exemplify as mixed type inhibitors. With raising the nanofiller concentration in the

tested samples, the efficiency of inhibition rises and reduces with rising temperature, and blend polymer/ 3% Au nanoparticles inhibitor has further tendency for corrosion inhibition.

The adsorption of the polymers under study onto the steel surface was used to dispute the inhibitory mechanism. A fine arrangement was established within the quantum chemical parameters (DFT and Mulliken atomic charges) and the experimental calculations. The inhibition efficiency of the present nanocomposite attained 91.3% and 89.0 % at room temperature using potentiodynamic polarization and EIS measurements, respectively. This makes our nanocomposite superior to similar materials and suggests using it as an inhibitor of corrosion.

#### Disclosure

This research did not receive any specific grant from funding agencies in the public, commercial or not-for-profit sectors. There is no Conflict of Interest

#### References

- Abdallah, Y. M., and K. Shalabi. "Comprehensive study of the behavior of copper inhibition in 1 M HNO<sub>3</sub> by Euphorbia helioscopia linn. extract as green inhibitor." *Protection of Metals and Physical Chemistry of Surfaces* 51.2 (2015): 275-284.
- Abdallah, Y. M., et al. "The Effect of TiB<sub>2</sub> on Electrochemical Performance of Udimet 700 Alloy in 1 M Hydrochloric Acid Solution and Its Corrosion Inhibition Using Some Organic Derivatives." *Protection of Metals and Physical Chemistry of Surfaces* 56.5 (2020): 1051-1065.
- Abdallah, Y. M., Shalabi, K. and Bayoumy. Nesma M. "Eco-friendly synthesis, biological activity and evaluation of some new pyridopyrimidinone derivatives as corrosion inhibitors for API 5L X52 carbon steel in 5% sulfamic acid medium." *Journal of Molecular Structure* 1171 (2018): 658-671.
- ABDEL-FATAH, HESHAM TM, et al. "Corrosion inhibition of mild steel in acidic medium by *Salvadora persica* (Miswak)–Part I: in sulfamic acid." *Chemical Science* 3.1 (2014): 221-231.
- Abdel-Fatah, Hesham TM, et al. "Effect of Tryptophan on the corrosion behavior of low alloy steel in sulfamic acid." *Arabian Journal of Chemistry* 9 (2016): S1069-S1076.
- Abdel-Rehim, S. S., K. F. Khaled, and N. S. Abd-Elshafi. "Electrochemical frequency modulation as a new technique for monitoring corrosion inhibition of iron in acid media by new thiourea derivative." *Electrochimica Acta* 51.16 (2006): 3269-3277.
- Ahamad, Ishtiaque, and M. A. Quraishi. "Mebendazole: new and efficient corrosion inhibitor for mild steel in acid medium." *Corrosion science* 52.2 (2010): 651-656.
- Askari, M., Aliofkhaezai, M. and Afroukhteh. S. "A comprehensive review on internal corrosion and cracking of oil and gas pipelines." *Journal of Natural Gas Science and Engineering* 71 (2019): 102971.
- Dehghani, Ali, et al. "Fabrication of metal-organic based complex film based on three-valent samarium ions-[bis (phosphonomethyl) amino] methylphosphonic acid (ATMP) for effective corrosion inhibition of mild steel in simulated seawater." *Construction and Building Materials* 239 (2020): 117812.
- Deng, Shuduan, Xianghong Li, and Xiaoguang Xie. "Hydroxymethyl urea and 1, 3-bis (hydroxymethyl) urea as corrosion inhibitors for steel in HCl solution." *Corrosion Science* 80 (2014): 276-289.
- Elashmawi, I. S., E. M. Abdelrazek, and A. Y. Yassin. "Influence of NiCl<sub>2</sub>/CdCl<sub>2</sub> as mixed filler on structural, thermal and electrical properties of PVA/PVP blend." *British Journal of Applied Science & Technology* 4.30 (2014): 4263.

- Farea, M. O., Abdelghany, A. M. and Oraby. A. H. "Optical and dielectric characteristics of polyethylene oxide/sodium alginate-modified gold nanocomposites." RSC advances 10.62 (2020): 37621-37630.
- Farea, M. O., Abdelghany, A. M. and Oraby. A. H. "Optical and dielectric characteristics of polyethylene oxide/sodium alginate-modified gold nanocomposites." RSC advances 10.62 (2020): 37621-37630.
- Gao, Guo, and Chenghao Liang. "Electrochemical and DFT studies of  $\beta$ -amino-alcohols as corrosion inhibitors for brass." *Electrochimica Acta* 52.13 (2007): 4554-4559.
- Garcia-Cabezon, C., et al. "Nanocomposites of conductive polymers and nanoparticles deposited on porous material as a strategy to improve its corrosion resistance." *Surface and Coatings Technology* 403 (2020): 126395.
- Gece, Gökhan, and Semra Bilgiç. "Quantum chemical study of some cyclic nitrogen compounds as corrosion inhibitors of steel in NaCl media." *Corrosion Science* 51.8 (2009): 1876-1878.
- Hsissou, Rachid, et al. "Evaluation of corrosion inhibition performance of phosphorus polymer for carbon steel in [1 M] HCl: Computational studies (DFT, MC and MD simulations)." *Journal of Materials Research and Technology* 9.3 (2020): 2691-2703.
- Ijaola, Ahmed Olanrewaju, Peter Kayode Farayibi, and Eylem Asmatulu. "Superhydrophobic coatings for steel pipeline protection in oil and gas industries: A comprehensive review." *Journal of Natural Gas Science and Engineering* 83 (2020): 103544.
- Jayaraman, R., et al. "AC impedance, XRD, DSC, FTIR studies on PbTiO<sub>3</sub> dispersoid pristine PVdF-co-HFP and PEMA blended PVdF-co-HFP microcomposite electrolytes." *Journal of Non-Crystalline Solids* 435 (2016): 27-32.
- Jeyaraj, T., et al. "2', 3-Dicarboxylato-4-Hydroxyazobenzene as corrosion inhibitor for aluminium in sodium hydroxide." *Transactions of the SAEST* 40.4 (2005): 139-145.
- Krumenacker, S. "Hearing aid dispensing training manual (2<sup>nd</sup> edition), San Diego, CA., Plural Publishing, Inc. (2019) : 138.
- Kumar, A. Madhan, and Zuhair M. Gasem. "In situ electrochemical synthesis of polyaniline/f-MWCNT nanocomposite coatings on mild steel for corrosion protection in 3.5% NaCl solution." *Progress in Organic Coatings* 78 (2015): 387-394.
- Lagreenee, M., et al. "Study of the mechanism and inhibiting efficiency of 3, 5-bis (4-methylthiophenyl)-4H-1, 2, 4-triazole on mild steel corrosion in acidic media." *Corrosion Science* 44.3 (2002): 573-588.
- Liu, Xin, Jihui Wang, and Wenbin Hu. "Preparation and inhibition behavior of Fe<sub>3</sub>O<sub>4</sub>/MBT nanocomposite inhibitor for mild steel in NaCl solution." *Colloids and Surfaces A: Physicochemical and Engineering Aspects* 613 (2021): 126088.
- Lukovits, I., E. Kalman, and F. Zucchi. "Corrosion inhibitors—correlation between electronic structure and efficiency." *Corrosion* 57.1 (2001): 3-8.
- Madkour, Loutfy H., Savaş Kaya, and Ime Bassey Obot. "Computational, Monte Carlo simulation and experimental studies of some arylazotriazoles (AATR) and their copper complexes in corrosion inhibition process." *Journal of Molecular Liquids* 260 (2018): 351-374.

- Mert, Başak Doğru, et al. "Inhibition effect of 2-amino-4-methylpyridine on mild steel corrosion: experimental and theoretical investigation." *Corrosion science* 85 (2014): 287-295.
- Mohan, K. Rama, et al. "Electrical and optical properties of (PEMA/PVC) polymer blend electrolyte doped with NaClO<sub>4</sub>." *Polymer testing* 30.8 (2011): 881-886.
- Mohanty, Fanismita, and Sarat K. Swain. "Nano silver embedded starch hybrid graphene oxide sandwiched poly (ethylmethacrylate) for packaging application." *Nano-Structures & Nano-Objects* 18 (2019): 100300.
- Morad, M. S. "Corrosion inhibition of mild steel in sulfamic acid solution by S-containing amino acids." *Journal of Applied Electrochemistry* 38.11 (2008): 1509-1518.
- Motamedi, M., Ali Reza Tehrani-Bagha, and M. Mahdavian. "Effect of aging time on corrosion inhibition of cationic surfactant on mild steel in sulfamic acid cleaning solution." *Corrosion Science* 70 (2013): 46-54.
- MubarakAli, D., et al. "Plant extract mediated synthesis of silver and gold nanoparticles and its antibacterial activity against clinically isolated pathogens." *Colloids and Surfaces B: Biointerfaces* 85.2 (2011): 360-365.
- Negm, Nabel A., and Ismail A. Aiad. "Synthesis and characterization of multifunctional surfactants in oil-field protection applications." *Journal of surfactants and detergents* 10.2 (2007): 87-92.
- Obaid, A. Y., et al. "Corrosion inhibition of type 430 stainless steel in an acidic solution using a synthesized tetra-pyridinium ring-containing compound." *Arabian journal of chemistry* 10 (2017): S1276-S1283.
- Obot, I. B., D. D. Macdonald, and Z. M. Gasem. "Density functional theory (DFT) as a powerful tool for designing new organic corrosion inhibitors. Part 1: an overview." *Corrosion Science* 99 (2015): 1-30.
- Oguzie, E. E., et al. "Evaluation of the inhibitory effect of methylene blue dye on the corrosion of aluminium in hydrochloric acid." *Materials Chemistry and Physics* 87.2-3 (2004): 394-401.
- Palaniappan, N., I. S. Cole, and A. E. Kuznetsov. "Experimental and computational studies of graphene oxide covalently functionalized by octylamine: electrochemical stability, hydrogen evolution, and corrosion inhibition of the AZ13 Mg alloy in 3.5% NaCl." *RSC advances* 10.19 (2020): 11426-11434.
- Prabhu, R. A., et al. "Inhibition effects of some Schiff's bases on the corrosion of mild steel in hydrochloric acid solution." *Corrosion Science* 50.12 (2008): 3356-3362.
- Premila, R., S. Rajendran, and K. Kesavan. "Influence of Blend on the Conductivity in Poly (Ethyl Methacrylate)/Poly (Vinyl Acetate) Based Polymer Electrolytes." *Nano Hybrids and Composites*. Vol. 17. Trans Tech Publications Ltd, 2017.
- Radhamani, A. V., Hon Chung Lau, and S. Ramakrishna. "Nanocomposite coatings on steel for enhancing the corrosion resistance: A review." *Journal of Composite Materials* 54.5 (2020): 681-701.
- Rosalbino, Francesco, et al. "EIS study on the corrosion performance of a Cr (III)-based conversion coating on zinc galvanized steel for the automotive industry." *Journal of Solid State Electrochemistry* 15.4 (2011): 703-709.
- Shalabi, K., Abdallah, Y. M. and Fouda. A. S. "Corrosion inhibition of aluminum in 0.5 M HCl solutions containing phenyl sulfonylacetophenoneazo derivatives." *Research on Chemical Intermediates* 41.7 (2015): 4687-4711.
- Shalabi, K., et al. "Adsorption and corrosion inhibition of Atropa belladonna extract on carbon steel in 1 M HCl solution." *Int. J. Electrochem. Sci* 9.3 (2014): 1468-1487.

- Yassin, A. Y., and A. M. Abdelghany. "Synthesis and thermal stability, electrical conductivity and dielectric spectroscopic studies of poly (ethylene-co-vinyl alcohol)/graphene oxide nanocomposite." *Physica B: Condensed Matter* 608 (2021): 412730.
- Yassin, A. Y., et al. "Enhancement of dielectric properties and AC electrical conductivity of nanocomposite using poly (vinyl chloride-co-vinyl acetate-co-2-hydroxypropyl acrylate) filled with graphene oxide." *Journal of Materials Science: Materials in Electronics* 29.18 (2018): 15931-15945.
- Zachariah, Susan, and Ying-Ling Liu. "Nanocomposites of polybenzoxazine-functionalized multiwalled carbon nanotubes and polybenzoxazine for anticorrosion application." *Composites Science and Technology* 194 (2020): 108169.
- Zain, N. F., et al. "Improvement of electrical conductivity of PEMA film by incorporating EMITFSI and carbon based nanofiller." *Organic Electronics* 78 (2020): 105562.
- Zhai, Qian, et al. "Estimation of wetting hydraulic conductivity function for unsaturated sandy soil." *Engineering Geology* 285 (2021): 106034.
- Zhang, Lei, et al. "Thermal Properties of Poly (vinyl chloride-co-vinyl acetate-co-2-hydroxypropyl acrylate)(PVVH) Polymer and Its Application in ZnO Based Nanogenerators." *Chinese Physics Letters* 28.1 (2011): 016501.
- Zhou, Weimin, et al. "Characterization of anti-adhesive self-assembled monolayer for nanoimprint lithography." *Applied Surface Science* 255.5 (2008): 2885-2889.